

# Simulation of noisy quantum circuits using frame representations

Janek Denzler,<sup>1</sup> Jose Carrasco,<sup>1</sup> Jens Eisert,<sup>1</sup> and Tommaso Guaita<sup>1,\*</sup>

<sup>1</sup>*Dahlem Center for Complex Quantum Systems, Freie Universität Berlin, 14195 Berlin, Germany*

(Dated: January 8, 2026)

One of the core research questions in the theory of quantum computing is to find out to what precise extent the classical simulation of a noisy quantum circuits is possible and where potential quantum advantages can set in. In this work, we introduce a unified framework for the classical simulation of quantum circuits based on frame theory, encompassing and generalizing a broad class of existing simulation strategies. Within this framework, the computational cost of a simulation algorithm is determined by the one-norm of an associated quasi-probability distribution, providing a common quantitative measure across different simulation approaches. This enables a comprehensive perspective on common methods for the simulation of noisy circuits based on different quantum resources, such as entanglement or non-stabilizerness. It further provides a clear scheme for generating novel classical simulation algorithms. Indeed, by exploring different choices of frames within this formalism and resorting to tools of convex optimization, we are able not only to obtain new insights and improved bounds for existing methods – such as stabilizer state simulation or Pauli back-propagation – but also to discover a new approach with an improved performance based on a generalization of the Pauli frame. We, thereby, show that classical simulation techniques can directly benefit from a perspective – that of frames – that goes beyond the traditional classification of quantum resources.

## I. INTRODUCTION

The classical simulation of quantum devices plays a central role in understanding the delicate boundary between classical and quantum computational power. A wealth of methods have been developed to simulate quantum circuits on classical hardware, each grounded in different operational pictures of quantum mechanics and tailored to specific computational goals. In this work, we present a framework, based on so-called *frame theory* [1–4], that is able to capture a comprehensive range of such methods and provides a conceptually clear and quantitatively simple way of characterizing their performance. This framework further suggests a well-defined path for generating novel simulation methods. We directly exploit this by constructing several new examples of frame-based methods. Some of these attain improved performance over previously known algorithms, demonstrating that this is an open direction where significant progress can still be expected.

On the highest level, one can differentiate simulation tasks based on the answer to the fundamental question: what does it mean to simulate a quantum computation classically? This answer may include estimating expectation values of observables, computing output probabilities (strong simulation), or sampling from the output distributions (weak simulation). Then, one may also broadly distinguish simulation approaches based on whether they adhere to the Schrödinger or Heisenberg picture.

In the Schrödinger picture, the focus is on constructing classical representations of the evolving quantum state.

These representations — ranging from tensor networks such as *matrix product states* (MPS) and *matrix product operators* (MPO) [5, 6] to linear combinations of polynomially many algebraically defined structures such as stabilizer states [7, 8], Gaussian states [9, 10], etc. — serve as a basis for estimating observables or reproducing output distributions. Each of these cases poses its own computational challenges and is sensitive to the structure of the quantum state. Conversely, simulation methods based on the Heisenberg picture target the evolution of observables rather than states. These include prominent techniques such as operator back-propagation, which are particularly effective for the estimation of expectation values of Pauli strings [11–16]. Despite their substantial conceptual differences, these approaches exhibit a shared behaviour: the classical cost of simulation grows exponentially with certain quantifiers of “quantumness” — be it entanglement, magic, coherence, non-Gaussianity, etc. Simulation is therefore classically efficient only if these resources remain logarithmically bounded in system size.

The presence of noise, however, complicates this landscape. Intuitively, as noise levels increase, quantum computations lose their advantage and become more amenable to classical simulation (although in practical situations it may not always be obvious how to leverage the noise to simplify simulation). This leads to the notion of an inverse threshold: a critical error rate  $p_{\text{cl}}$  above which a quantum computation becomes efficiently simulable classically, regardless of the intrinsic quantum resources it employs. This concept stands in contrast to the traditional error-correction threshold  $p_{\text{ec}}$ , below which fault-tolerant quantum computation becomes possible. Importantly, the inverse threshold is not universal — it depends both on the noise model and on the specific type of simulation under consideration, whether strong, weak, or expectation-value-based. We further note that

---

\* [tommaso.guaita@fu-berlin.de](mailto:tommaso.guaita@fu-berlin.de)

to date most insights into circuit simulability have been derived in an average-case setting, involving ensembles of random circuits in certain architectures — typically brick-wall structures, local connectivity in one dimension, *etc.*

Within this classical simulation context, this work focuses on the task of computing observable expectations up to additive precision. We employ for this a unifying framework based on frame theory, adapting it explicitly to the simulation of noisy quantum circuits, both in the Schrödinger and in the Heisenberg picture. This offers a structured and comprehensive perspective on classical simulation across different pictures, strategies and types. Indeed, we show that many of the existing methods can be interpreted as specific instances of a broader class of simulation strategies, each characterized by different choices of *frame*. Crucially, from this point of view, the efficiency of a simulation algorithm is directly related to the efficiency of a simple Monte Carlo sampling process (constructed from the given frame representation), which can be straightforwardly analyzed. We use this fact to derive inverse thresholds for individual circuits composed from common gate-sets, without relying on statistical averaging over circuit ensembles.

Furthermore, this perspective reveals that we are not bound to the traditional choices of frames (Pauli operators, stabilizer states, *etc.*), but there is rather a broad and so far mostly unexplored space for developing novel simulation methods based on alternative frame choices. We demonstrate that exploring this space is a worthwhile endeavour by proposing two new frames based on product operators that provably improve on the performance of existing methods, both in the Schrödinger and in the Heisenberg picture.

After an introductory overview of the classical simulation framework (in Section II) and of the frame theory perspective (in Section III), we present the following main results. First, in Section IV, we analyse in depth two frames based on stabilizer states previously introduced in Ref. [4], showing how to compute their performance for the simulation of arbitrary noisy gate-sets using convex optimization tools that we develop. We then complete our discussion of simulation methods in the Schrödinger picture by introducing a novel frame based on product states. Finally, in Section V, we move to simulation methods in the Heisenberg picture, discussing how and why they can circumvent some limitations of the Schrödinger picture methods. Here, we first discuss from our perspective the well-established Pauli frame. Then we proceed to introduce a generalization of the Pauli frame, which shows a reduced simulation cost under certain noise models.

## II. PRELIMINARIES ON CLASSICAL SIMULATION

Among the different possible definitions of classical simulation, in this work we are specifically interested in the following setting. We consider quantum circuits composed of a polynomial number of gates chosen from a fixed gate-set, composed of gates acting on a constant number of qubits (usually one and two qubit gates). We will generally consider universal unitary gate-sets (*e.g.*, Clifford+ $T$ ).

On top of this, we then assume that the gates from the given gate-set may be noisy. This means that each gate is replaced by a non-unitary quantum channel only approximately close to the target unitary gate. Usually, we will construct these noisy gates by composing the unitary channel with a standard noise channel (*e.g.*, depolarizing noise) parametrised by a noise strength  $p$ . However one can also straightforwardly consider more general scenarios, as we shall see.

Once this noisy gate-set is fully specified, the problem is then well identified: we consider all possible circuits that can be built by concatenating  $m = \text{poly}(n)$  such noisy gates on  $n$  qubits. Note, in particular, that we do not make any further assumptions on the circuit architecture: we do not require a specific connectivity, nor that the noise is applied uniformly to all qubits after each circuit layer, nor do we rule out the introduction of fresh qubits during the circuit.

For any such given circuit the task is to compute, with classical computational resources, the expectation value of a specific observable  $O$ . That is, to compute

$$\langle O \rangle = \text{tr}[O \mathcal{C}_m \circ \dots \circ \mathcal{C}_1(\rho_0)], \quad (1)$$

where  $\mathcal{C}_1, \dots, \mathcal{C}_m$  are the channels representing the  $m$  noisy gates in the circuit and  $\rho_0$  is a fixed initial state (usually the  $|0^n\rangle$  state). We further assume that it is sufficient to compute this expectation value to within an additive error  $\epsilon$ . We say an algorithm for this task is *efficient* if its runtime scales as  $\text{poly}(n, m, 1/\epsilon)$ .

Having introduced the simulation problem that we will be addressing, let us briefly comment on its relation to other notions of simulation that are commonly discussed in the literature [8]. First, we stress that we are interested in the simulation of expectation values to additive precision. This is different from so-called *strong simulation* (*i.e.*, computing with sufficient precision the amplitudes  $\langle o_1, \dots, o_n | \psi \rangle$ , where  $|o_1, \dots, o_n\rangle$  are mutual eigenvectors of some commuting observables  $O_1, \dots, O_n$  and  $|\psi\rangle$  is the output state vector of the circuit) and from *weak simulation* (*i.e.*, sampling from the distribution  $p(o_1, \dots, o_n) = |\langle o_1, \dots, o_n | \psi \rangle|^2$ ). While weak and strong simulation are mutually inequivalent tasks, efficient weak simulation does imply efficient simulation of expectation values to additive precision. Weak simulation is also the most natural definition of what it means to simulate an actual quantum computer (which ultimately

just outputs samples from a certain measurement outcome distribution) [17, 18]. Nonetheless, simulation of expectation values is still an interesting and non-trivial task in itself as, for instance, estimating the expectation of a single observable on an arbitrary circuit is a BQP-complete problem.

Second, we note that many relevant recent results in the field of classical simulation of (noisy) quantum circuits are statements on the *average case* simulability of ensembles of random circuits [5, 11–14, 19, 20]. That is, they state that if one samples a random circuit from a given ensemble, it will be with high probability a circuit that can be efficiently simulated classically. This type of results however says nothing about the small, but possibly relevant, set of circuits that are excluded by this “high probability” statement. In this work, in contrast, we are instead focusing on *worst case* statements. That is, we want to make statements on the simulability of all circuits that can be generated by one of the noisy gate-sets introduced above.

### III. SIMULATION WITH FRAMES AND QUASI-PROBABILITIES

The main results of this work will be to introduce and analyse several methods for the classical simulation task defined above. All these methods can be collectively understood as instances of a more general simulation framework which we refer to as “quasi-probability simulation with quantum frames”. In this section, we therefore first give a comprehensive and self-contained presentation of this framework, whose main elements have been previously introduced in Refs. [1, 3]. A schematic representation of the simulation algorithms in the frame theory framework can be found in Figure 1.

The main object that characterises any method in this framework is a so-called *frame*. A frame  $\mathcal{F}$  is a set of operators which spans the whole space  $\mathcal{L}(\mathcal{H})$  of linear operators on the system’s Hilbert space  $\mathcal{H}$ . That is

$$\mathcal{F} = \{F_x, \forall x \in \mathcal{X}\}, \quad (2)$$

where  $\mathcal{X}$  is an arbitrary set of indices and  $F_x \in \mathcal{L}(\mathcal{H})$  are such that any linear operator  $A \in \mathcal{L}(\mathcal{H})$  can be written as

$$A = \sum_{x \in \mathcal{X}} \lambda_x^A F_x \quad (3)$$

for some set of complex coefficients  $\{\lambda_x^A\}_{x \in \mathcal{X}}$ .

A particular example of a frame would be a basis of  $\mathcal{L}(\mathcal{H})$  such as, for instance, the Pauli basis for the space of operators on a  $n$ -qubit system  $\mathcal{H} = (\mathbb{C}^2)^{\otimes n}$ . However, we do not necessarily require frames to be bases and, in particular, we do not require the frame elements  $F_x$  to be all linearly independent. It follows that a frame could also be an overcomplete set of linear generators of  $\mathcal{L}(\mathcal{H})$  and that the expression (3) does not uniquely identify

the coefficients  $\lambda_x^A$ , rather there could exist many choices of  $\lambda_x^A$  that represent the same operator  $A$ .

Given a frame, we can use it to represent not only operators in  $\mathcal{L}(\mathcal{H})$  but also superoperators (*i.e.*, maps from  $\mathcal{L}(\mathcal{H})$  to itself, such as quantum channels). A superoperator  $\mathcal{C}$  will be represented by a “matrix” of coefficients  $\lambda_{x,y}^{\mathcal{C}}$  depending on two frame indices such that

$$\mathcal{C}(F_x) = \sum_{y \in \mathcal{X}} \lambda_{x,y}^{\mathcal{C}} F_y \quad (4)$$

for all  $x \in \mathcal{X}$ . Again, note that this representation is in general not unique.

#### A. Circuit evolution with frames

The main idea of the quasi-probability method is to consider expression (1) and represent either the state or the observable as it evolves through the circuit by expanding it on the frame elements. To make this more concrete, we will for now consider the case in which we represent the evolution of the state (*i.e.*, the Schrödinger picture), but we will later comment on how the same concept can be applied also to representing the evolution of the observable (*i.e.*, the Heisenberg picture).

In a given frame  $\mathcal{F}$ , the initial state  $\rho_0$  admits a decomposition  $\rho_0 = \sum_{x \in \mathcal{X}} \lambda_x^{\rho_0} F_x$ . Substituting this into equation (1) gives

$$\langle O \rangle = \sum_{x \in \mathcal{X}} \lambda_x^{\rho_0} \text{tr}[O \mathcal{C}_m \circ \cdots \circ \mathcal{C}_1(F_x)]. \quad (5)$$

We can now imagine to also have access to frame decompositions of the form (4) for all the channels  $\mathcal{C}_j$  and substitute these in turn into the expression above. This leads to

$$\langle O \rangle = \sum_{x_1, \dots, x_{m+1}} \lambda_{x_1}^{(0)} \lambda_{x_1, x_2}^{(1)} \cdots \lambda_{x_m, x_{m+1}}^{(m)} \text{tr}[O F_{x_{m+1}}], \quad (6)$$

where to simplify the notation we have used the shorthand  $\lambda_x^{(0)} \equiv \lambda_x^{\rho_0}$  and  $\lambda_{x,y}^{(j)} \equiv \lambda_{x,y}^{\mathcal{C}_j}$ . Note that we are here assuming that one can always find and write down these frame decompositions: we will later discuss in detail what conditions need to be satisfied such that there is actually an efficient algorithm for this, but we will for now postpone this issue to focus first on the general idea.

The expression (6) is nothing but an equivalent rewriting of (1). The sum over  $x_1, \dots, x_{m+1}$  runs over a number of terms exponentially large in  $m$ , even if each  $x_j$  only takes a small constant number of values. So evaluating directly the sum in (6) does not lead to an efficient simulation of the expectation value. The idea, however, is to observe that, if we are only interested in estimating  $\langle O \rangle$  to additive precision, then it might be sufficient to only consider a small stochastically sampled subset of terms of the sum.

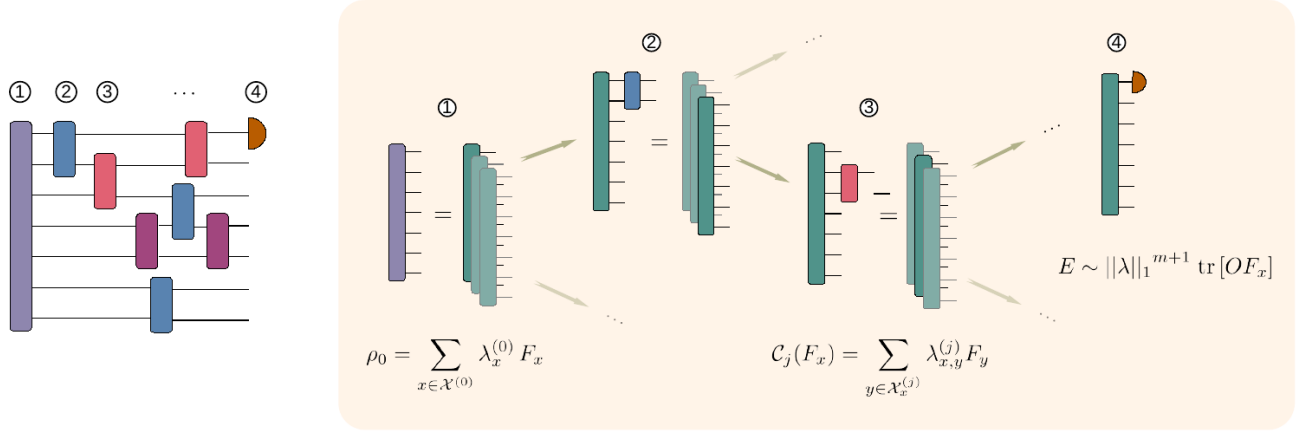


FIG. 1. A schematic representation of a simulation algorithm based on the frame theory framework (represented here in the Schrödinger picture for illustration purposes). A path of frame elements is generated by sampling at each step a new element, based on the frame decomposition of the circuit gate acting on the previous element. At the final step, an estimator  $E$  is evaluated, whose range – and thus its sample complexity – depends on the quantity  $\|\lambda\|_1^{m+1}$ .

To put this Monte Carlo idea into practice, we need to identify some natural probability distribution to sample from. We do this by expressing each complex number

$\lambda_{x,y}^{(j)}$  as a product of its modulus  $|\lambda_{x,y}^{(j)}|$  and a complex phase  $\varphi_{x,y}^{(j)}$ . With this notation we can write

$$\langle O \rangle = \sum_{x_1, \dots, x_{m+1}} |\lambda_{x_1}^{(0)}| |\lambda_{x_1, x_2}^{(1)}| \dots |\lambda_{x_m, x_{m+1}}^{(m)}| \text{tr}[O F_{x_{m+1}}] \varphi_{x_1}^{(0)} \varphi_{x_1, x_2}^{(1)} \dots \varphi_{x_m, x_{m+1}}^{(m)} \quad (7)$$

$$= \sum_{x_1, \dots, x_{m+1}} \frac{|\lambda_{x_1}^{(0)}|}{\sum_{x'_1} |\lambda_{x'_1}^{(0)}|} \frac{|\lambda_{x_1, x_2}^{(1)}|}{\sum_{x'_2} |\lambda_{x_1, x'_2}^{(1)}|} \dots \frac{|\lambda_{x_m, x_{m+1}}^{(m)}|}{\sum_{x'_{m+1}} |\lambda_{x_m, x'_{m+1}}^{(m)}|} E_{x_1, \dots, x_{m+1}}$$

where in the second step we have just multiplied and divided by the normalisation terms  $\sum_{x'_{j+1}} |\lambda_{x_j, x'_{j+1}}^{(j)}|$  and then collected several factors into the quantity

$$E_{x_1, \dots, x_{m+1}} := \text{tr}[O F_{x_{m+1}}] \varphi_{x_1}^{(0)} \varphi_{x_1, x_2}^{(1)} \dots \varphi_{x_m, x_{m+1}}^{(m)} \left( \sum_{x'_1} |\lambda_{x'_1}^{(0)}| \right) \left( \sum_{x'_2} |\lambda_{x_1, x'_2}^{(1)}| \right) \dots \left( \sum_{x'_{m+1}} |\lambda_{x_m, x'_{m+1}}^{(m)}| \right). \quad (8)$$

We now observe that the following objects are well-defined probability distributions

$$p_0(x) = \frac{|\lambda_x^{(0)}|}{\sum_{x'} |\lambda_{x'}^{(0)}|}, \quad (9)$$

$$p_j(x|y) = \frac{|\lambda_{y,x}^{(j)}|}{\sum_{x'} |\lambda_{y,x'}^{(j)}|}, \quad \text{for } j = 1, \dots, m, \quad (10)$$

namely they are positive and normalised as  $\sum_x p_0(x) =$

$\sum_x p_j(x|y) = 1$ . This allows us to finally write

$$\begin{aligned} \langle O \rangle &= \sum_{x_1, \dots, x_{m+1}} p_0(x_1) \dots p_m(x_{m+1}|x_m) E_{x_1, \dots, x_{m+1}} \quad (11) \\ &= \mathbb{E}[E_{x_1, \dots, x_{m+1}}], \end{aligned}$$

where  $\mathbb{E}$  denotes an expectation value with respect to the probability distribution

$$p(x_1, \dots, x_{m+1}) = p_0(x_1) p_1(x_2|x_1) \dots p_m(x_{m+1}|x_m). \quad (12)$$

This allows us to conclude that we can evaluate the expectation value  $\langle O \rangle$  just by drawing samples  $(x_1, \dots, x_{m+1})$  from the distribution  $p(x_1, \dots, x_{m+1})$  and computing the average value of the corresponding random variable  $E_{x_1, \dots, x_{m+1}}$ . The structure of the probability distribution (12), which is expressed as a product of conditional probabilities, implies that we can draw each sample according to the following protocol: we first sample  $x_1$  from the distribution  $p_0(x_1)$ , then we sample  $x_2$  from the distribution  $p_1(x_2|x_1)$  where  $x_1$  has been fixed to the value that we sampled at the previous step, and so on for the rest of  $x_3, \dots, x_m$ .

After sampling  $N$  such samples, which we label as  $(x_1^{(k)}, \dots, x_{m+1}^{(k)})$  for  $k = 1, \dots, N$ , we can estimate the average value as

$$\tilde{E} = \frac{1}{N} \sum_j E_{x_1^{(k)}, \dots, x_{m+1}^{(k)}}. \quad (13)$$

As one increases the number of samples  $N$  this estimate will converge to the value of  $\langle O \rangle$ . The remaining question is how many such samples are needed to obtain a sufficiently precise estimate. This can be addressed by using the Hoeffding inequality [21], which states that to obtain an estimate that is within precision  $\epsilon$  with probability at least  $1 - \delta$ , one needs to take  $N$  samples with

$$N = \frac{2 \log(2/\delta)}{\epsilon^2} |E|^2, \quad (14)$$

where we have defined  $|E| := \sup_{x_1, \dots, x_{m+1}} |E_{x_1, \dots, x_{m+1}}|$ .

We see, therefore, that the number of required samples, and thus also the runtime of the simulation algorithm, will depend crucially on  $|E|$ , *i.e.*, the range of the random variable  $E_{x_1, \dots, x_{m+1}}$ . To simplify the following expressions we introduce here a one-norm notation

$$\|\lambda^{(0)}\|_1 := \sum_{x'} |\lambda_{x'}^{(0)}|, \quad (15)$$

$$\|\lambda_x^{(j)}\|_1 := \sum_{x'} |\lambda_{x,x'}^{(j)}|, \quad \text{for } j = 1, \dots, m \quad (16)$$

to indicate the normalisation terms appearing in  $|E|$ . We can then estimate  $|E|$  as

$$\begin{aligned} |E| &= \sup_{x_1, \dots, x_{m+1}} |\text{tr} [OF_{x_{m+1}}]| \|\lambda^{(0)}\|_1 \|\lambda_{x_1}^{(1)}\|_1 \cdots \|\lambda_{x_m}^{(m)}\|_1 \\ &\leq \|\lambda\|_1^{m+1} \sup_x |\text{tr} [OF_x]|, \end{aligned} \quad (17)$$

where in the second step (17) we have derived an upper-bound by defining the maximal one-norm value over all inputs and all gates as

$$\|\lambda\|_1 := \max_j \|\lambda^{(j)}\|_1, \quad (18)$$

where

$$\|\lambda^{(j)}\|_1 := \sup_x \|\lambda_x^{(j)}\|_1, \quad \text{for } j = 1, \dots, m. \quad (19)$$

Comparing equations (17) and (14), we conclude that the number of iterations of the simulation algorithm will depend on the one-norm of the coefficients  $\lambda_{x,y}^{(j)}$  which represent the circuit gates in the chosen frame and in particular it will be bounded by  $O(\|\lambda\|_1^{2m})$ . That is, if  $\|\lambda\|_1 > 1$  then the algorithm's runtime can grow exponentially in the number of gates  $m$ . On the other hand the runtime will remain bounded in  $m$  if, for each gate in the circuit and for each input index  $x$ , the one-norm  $\|\lambda_x^{(j)}\|_1$  is upper bounded by 1. Notice further that, if only a subset of gates in the gate-set has  $\|\lambda^{(j)}\|_1 > 1$ , then the cost of the algorithm scales exponentially in the number of these “difficult to simulate” gates (and not in the total number of gates  $m$ ).

Finally, the following observation will be crucial for the results presented later. We have so far simply assumed that we choose a set of coefficients  $\lambda_{x,y}^{(j)}$  that satisfy (4) for all the gates in the circuit. For any such choice, the analysis above is valid and the resulting algorithm will have a runtime depending on the value of  $\|\lambda\|_1$  for this specific choice. We note, however, that for general frames the choice of coefficients is not unique, so there is a certain freedom in the algorithm design depending on this choice. It is then clear that, ideally, one should choose, among all possible decompositions of each circuit gate, the ones that give the minimal value of  $\|\lambda^{(j)}\|_1$ . While it is true that efficiently solving this optimization problem is not always possible, it is nonetheless also true that any choice that improves the value of  $\|\lambda^{(j)}\|_1$  will correspondingly reduce the simulation cost. We will see in what follows that exploiting overcomplete frames to search for better decompositions can in fact be beneficial.

This is in a way analogous to what is referred to as the “easing” of the sign problem in standard Monte Carlo methods [22, 23]. Indeed, the overall structure of the above method – except for the use of frames – is very similar to the way Monte Carlo methods are commonly being used in the simulation of complex quantum systems [24]. If expressions such as Eq. (9) and (10) do not have a denominator, as  $\lambda_x^{(0)}$  and  $\lambda_{y,x}^{(j)}$  are readily non-negative and normalized, then one refers to the problem as a “sign-free” and efficient sampling is possible [24, 25]. If this is not the case, then the normalizations in Eq. (9) and (10) commonly lead to an exponential sample complexity. It is known that being sign-free is a basis dependent property [22, 23, 26, 27], so effort has been made to understand how to make problems sign-free by suitable basis choices or how to ease the sign problem, quantified in terms of one-norms, and what the precise computational complexity of this process is [22, 23, 27]. Here, we face a partially related task where the sampling overhead is reduced by searching for optimal representations in a fixed frame, which possibly encompasses many bases at the same time.

## B. Simulation in the Schrödinger picture

In the previous discussion we have discussed the general idea of how a stochastic Monte Carlo algorithm for circuit expectation values can be derived by representing the circuit on a chosen frame. We have shown how in principle the algorithm's complexity will depend on the value of a certain one-norm of the coefficients representing the circuit's gates in the given frame. We will now discuss more in detail how an efficient classical simulation algorithm of this type can be defined in the Schrödinger picture.

First, we need a frame that can be efficiently represented classically. That is, we require that each frame element  $F_x$  is identified by a label  $x$  that can be expressed as a set of classical parameters of size at most  $\text{poly}(n)$ . Note that the total number of frame elements could nonetheless be exponentially large in  $n$  or, in principle, even infinite for continuous parametrizations.

Given the frame, we need to be able to decompose the initial state and each (noisy) gate of the circuit as linear combinations of some subset of frame elements, that is,

$$\rho_0 = \sum_{x \in \mathcal{X}^{(0)}} \lambda_x^{(0)} F_x, \quad (20)$$

$$\mathcal{C}_j(F_x) = \sum_{y \in \mathcal{X}_x^{(j)}} \lambda_{x,y}^{(j)} F_y \quad (21)$$

for all inputs  $F_x \in \mathcal{F}$ . Here  $\mathcal{X}^{(0)} \subseteq \mathcal{X}$  and  $\mathcal{X}_x^{(j)} \subseteq \mathcal{X}$  are subsets of indices that represent the support of each of these decompositions. A valid choice of decompositions (20) and (21) should be identifiable efficiently classically. That is, we require that both the supports  $\mathcal{X}^{(0)}$  and  $\mathcal{X}_x^{(j)}$  and the coefficients  $\lambda_x^{(0)}$  and  $\lambda_{x,y}^{(j)}$  should be classically efficiently computable in terms of the inputs  $x$  and  $y$ . We will further need to be able to efficiently sample elements out of these supports, according to probability distributions proportional to  $|\lambda_x^{(0)}|$  and  $|\lambda_{x,y}^{(j)}|$ . Various structures could lead to this property, but in most example that we treat this will be because the sets  $\mathcal{X}^{(0)}$  and  $\mathcal{X}_x^{(j)}$  only contain a constant number of elements in the system size  $n$ .

Finally, to evaluate the random variable  $E_{x_1, \dots, x_{m+1}}$ , we need to be able to compute  $\text{tr}[OF_x]$  for the observable of interest  $O$  and for any frame element  $F_x$ . This should be computable efficiently classically for any  $x$  and its value should be bounded, to prevent the range (17) from becoming inefficiently large. That is, we require

$$|\text{tr}[OF_x]| \leq \text{poly}(n) \quad \forall x \in \mathcal{X}. \quad (22)$$

A choice of frame that satisfies all the requirements above for the given circuit will produce a stochastic algorithm for the expectation value  $\langle O \rangle$ , according to the protocol discussed in the previous subsection. In this algorithm, each sample can be produced with a classically efficient runtime of order  $\text{poly}(n, m)$ . The total complex-

ity of the algorithm will then be determined by the required number of these samples, which, as we have discussed, will scale as  $O(\|\lambda\|_1^{2m})$  and thus depends on the value of  $\|\lambda\|_1$  of the considered gate decompositions (21).

## C. Simulation in the Heisenberg picture

A very similar analysis can be performed when treating the problem in the Heisenberg picture, that is rewriting (1) as

$$\langle O \rangle = \text{tr}[\rho_0(\mathcal{C}_1^* \circ \dots \circ \mathcal{C}_m^*(O))]. \quad (23)$$

Here,  $\mathcal{C}^*$  denotes the adjoint of the channel  $\mathcal{C}$  with respect to the Hilbert-Schmidt inner-product on  $\mathcal{L}(\mathcal{H})$ . The simulation algorithm is constructed completely analogously to before, by first decomposing  $O$  on the frame elements and then sequentially applying each gate  $\mathcal{C}_j^*$  and again decomposing the resulting outcome. The final estimator for the desired expectation value will have the form (8), where we replace  $\text{tr}[OF_{x_{m+1}}]$  by  $\text{tr}[\rho_0 F_{x_{m+1}}]$ .

Assume again to have a frame  $\mathcal{F}$  where each element can be labelled efficiently classically. The condition that we now require is that a choice of decompositions of the following form

$$O = \sum_{x \in \mathcal{X}^{(0)}} \lambda_x^{(0)} F_x, \quad (24)$$

$$\mathcal{C}_j^*(F_x) = \sum_{y \in \mathcal{X}_x^{(j)}} \lambda_{x,y}^{(j)} F_y, \quad (25)$$

can be identified efficiently classically as for all gates  $\mathcal{C}_j^*$  and all inputs  $F_x \in \mathcal{F}$ . We further require to be able to sample efficiently from the supports  $\mathcal{X}^{(0)}$  and  $\mathcal{X}_x^{(j)}$ , possibly because they all have a constant size. Finally, we require that the quantity  $\text{tr}[\rho_0 F_x]$  can be evaluated efficiently classically for all  $x \in \mathcal{X}$  and it satisfies

$$|\text{tr}[\rho_0 F_x]| \leq \text{poly}(n) \quad \forall x \in \mathcal{X}. \quad (26)$$

If all the requirements above are satisfied for the given circuit, then a stochastic algorithm for the expectation value  $\langle O \rangle$  exists, where each sample can be produced with a classically efficient runtime of order  $\text{poly}(n, m)$ . The total complexity of the algorithm will then be determined by the required number of these samples, which will scale as  $O(\|\lambda\|_1^{2m})$  and thus depends on the value of  $\|\lambda\|_1$  of the considered gate decompositions (25).

## IV. RESULTS IN THE SCHRÖDINGER PICTURE

A key feature of the general formalism introduced in the previous sections is that any definition of a frame leads to a different simulation method. Our main results are now derived by analysing in detail the algorithms that

can be constructed with some specific choices of frames. In this section, we focus on some frame choices suitable to be used in the Schrödinger picture, that is satisfying the requirements discussed in Section III B. We begin with two frames based on stabilizer states introduced in Refs. [4, 28], developing an explicit method for applying them to circuit simulation. We then also construct a new approach based on product state frames. In all these cases, we show explicitly how to optimize  $\|\lambda\|_1$  over frame decompositions.

### A. Stabilizer frames

Let us consider frames, suitable to be used in the Schrödinger picture, where the frame elements  $F_x$  are constructed out of stabilizer state vectors [29]. This can be done in two distinct ways.

#### 1. Diagonal stabilizer frame

First, we have the frame  $\mathcal{F} = \{F_x\}_{x \in \mathcal{X}}$  with frame elements of the form  $F_x = |\psi_x\rangle\langle\psi_x|$  for normalized stabilizer state vectors  $|\psi_x\rangle$  [28]. For example, for  $n = 1$  we have six elements  $|0\rangle\langle 0|$ ,  $|1\rangle\langle 1|$ ,  $|\pm\rangle\langle\pm|$ ,  $|\pm i\rangle\langle\pm i|$ , respectively the  $+1$  eigenstates of  $\pm Z, \pm X, \pm Y$ . In general, a stabilizer state vector  $|\psi_x\rangle$  on  $n$  qubits is identified by  $n$  signed Pauli operators that pairwise commute. Therefore it can be labelled by a string  $x$  of  $O(n^2)$  bits: this provides a classically efficient parametrisation of the frame. The total size of the frame is  $|\mathcal{X}| = 2^{O(n^2)}$  [29, 30].

First, we notice that  $\text{tr}[OF_x] = \langle\psi_x|O|\psi_x\rangle$  can be efficiently computed if the observable  $O$  is a Pauli operator [30]. Furthermore equation (22) is satisfied as

$$|\langle\psi_x|O|\psi_x\rangle| \leq \|O\|. \quad (27)$$

This makes the frame suitable for simulation in the Schrödinger picture. We therefore study Eqs. (15)-(16) which take the form

$$\rho_0 = \sum_{x \in \mathcal{X}^{(0)}} \lambda_x^{(0)} |\psi_x\rangle\langle\psi_x|, \quad (28)$$

$$\mathcal{C}_j(|\psi_x\rangle\langle\psi_x|) = \sum_{y \in \mathcal{X}_x^{(j)}} \lambda_{x,y}^{(j)} |\psi_y\rangle\langle\psi_y|. \quad (29)$$

For an initial stabilizer state such as  $\rho_0 = |0^n\rangle\langle 0^n|$ , a trivial decomposition (28) exists where  $\mathcal{X}^{(0)}$  contains a single element and  $\|\lambda^{(0)}\|_1 = 1$ .

Regarding the decomposition of gates, if a channel  $\mathcal{C}_j$  can be written as a convex combination of  $\text{poly}(n)$  unitary Clifford channels then one can efficiently find a decomposition (29) where  $\mathcal{X}_x^{(j)}$  contains polynomially many elements and  $\|\lambda_x^{(j)}\| = 1$ . More specifically, consider  $\mathcal{C}_j(\cdot) = \sum_k p_k C_k(\cdot) C_k^\dagger$ , where  $C_k$  are Clifford unitaries. Then, because Cliffords map stabilizer states to stabilizer

states,  $\mathcal{C}_j(|\psi_x\rangle\langle\psi_x|)$  is of the form (29) where the coefficients  $\lambda_{x,y}^{(j)}$  coincide with the positive normalised distribution  $p_k$ . It follows that this class of channels can be simulated with an efficient algorithm cost. For example, this is the case for any local Clifford gate affected by Pauli noise.

For what concerns general non-Clifford channels  $\mathcal{C}_j$ , we analyse here the case of single-qubit gates. Indeed, common gate-set choices require just one single-qubit non-Clifford gate, *e.g.*, the  $T$ -gate. Note, however, that the following analysis can be in principle generalized to the case of arbitrary local gates supported on a constant number  $q$  of qubits. Without loss of generality, we consider the action of a single-qubit channel  $\mathcal{C}_j = \mathcal{I}^{\otimes(n-1)} \otimes \mathcal{C}'_j$  acting on the last qubit of the system (channels acting on other qubits can be seen as permutations of this one, where permutations are Clifford operations).

We would now like to find decompositions of the form (29) for this channel  $\mathcal{C}_j$  which are optimal in the sense of having the lowest possible  $\|\lambda^{(j)}\|_1$ , as this corresponds to the lowest simulation cost. We are not going to solve this problem by searching over the space of all possible decompositions, but we will rather restrict ourselves to a subset of decompositions that can be treated efficiently. We do this by observing that any stabilizer state vector on  $n$  qubits can be efficiently written as

$$|\psi^{(n)}\rangle = (C^{(n-1)} \otimes I) |0^{n-2}\rangle |\psi^{(2)}\rangle \quad (30)$$

for some Clifford unitary  $C^{(n-1)}$  acting on  $n-1$  qubits and some 2-qubit stabilizer state vector  $|\psi^{(2)}\rangle$ . With this, we find that  $\mathcal{C}_j(|\psi_x\rangle\langle\psi_x|)$  is given by

$$\begin{aligned} \mathcal{C}_j(|\psi_x\rangle\langle\psi_x|) &= (C^{(n-1)} \otimes I) \\ &\times \left[ |0^{n-2}\rangle\langle 0^{n-2}| \otimes (\mathcal{I} \otimes \mathcal{C}'_j)(|\psi^{(2)}\rangle\langle\psi^{(2)}|) \right] (C^{(n-1)} \otimes I)^\dagger \end{aligned} \quad (31)$$

where we have exploited the single-qubit nature of the channel  $\mathcal{C}_j = \mathcal{I}^{\otimes(n-1)} \otimes \mathcal{C}'_j$  to commute it past the Clifford unitary. Thus, any decomposition of  $(I \otimes \mathcal{C}'_j)(|\psi^{(2)}\rangle\langle\psi^{(2)}|)$  over 2-qubit stabilizer states  $\{|\psi_y^{(2)}\rangle\langle\psi_y^{(2)}|\}$  will also give a decomposition of  $\mathcal{C}_j(|\psi_x\rangle\langle\psi_x|)$ , by substituting it into equation (31). Furthermore, the latter decomposition will have a value of  $\|\lambda_x^{(j)}\|_1$  equal to the one of the corresponding decomposition over 2-qubit stabilizer states. We can now therefore focus on searching for 2-qubit decompositions with the lowest possible  $\|\lambda_x^{(j)}\|_1$ .

It turns out that the solution of this restricted problem is actually optimal. Consider indeed an arbitrary decomposition of the form (29). Then, by comparing this to equation (31), we see that it must hold

$$\begin{aligned} &(\mathcal{I} \otimes \mathcal{C}'_j)(|\psi^{(2)}\rangle\langle\psi^{(2)}|) = \\ &= \sum_y \lambda_{x,y}^{(j)} \|\langle 0^{n-2}|(C^{(n-1)} \otimes I)^\dagger |\psi_y\rangle\|^2 |\tilde{\psi}_y^{(2)}\rangle\langle\tilde{\psi}_y^{(2)}|, \end{aligned} \quad (32)$$

where we have observed that

$$|\tilde{\psi}_y^{(2)}\rangle := \frac{\langle 0^{n-2}|(C^{(n-1)} \otimes I)^\dagger |\psi_y\rangle}{\|\langle 0^{n-2}|(C^{(n-1)} \otimes I)^\dagger |\psi_y\rangle\|} \quad (33)$$

are normalised 2-qubit stabilizer states. It therefore follows that, if a decomposition (29) exists, then there also exists a 2-qubit decomposition of  $(\mathcal{I} \otimes \mathcal{C}_j')(|\psi^{(2)}\rangle\langle\psi^{(2)}|)$  with one-norm upper-bounded by

$$\sum_y |\lambda_{x,y}^{(j)}| \|\langle 0^{n-2}|(C^{(n-1)} \otimes I)^\dagger |\psi_y\rangle\|^2 \leq \sum_y |\lambda_{x,y}^{(j)}|. \quad (34)$$

In conclusion, the result that we obtain by searching over 2-qubit decompositions cannot be worse than what one would find by searching over all possible decompositions.

More generally, for channels acting on a constant number of qubits  $q$ , with arguments analogous to the one above, one can restrict the problem to optimizing over stabilizer states of  $q+1$  qubits. If  $q$  is constant, this can be written as an efficiently solvable optimization problem, as we show in the following Section IV A 3 for the case  $q=1$ .

## 2. Dyadic stabilizer frame

The previously discussed diagonal stabilizer frame is a subset of the more general dyadic stabilizer frame [4]. This is the frame  $\mathcal{F} = \{F_{(x_1,x_2)}\}_{(x_1,x_2) \in \mathcal{X}}$  with frame elements of the form  $F_{(x_1,x_2)} = |\psi_{x_1}\rangle\langle\psi_{x_2}|$  for a pair of normalized stabilizer state vectors  $|\psi_{x_1}\rangle$  and  $|\psi_{x_2}\rangle$ . This frame also clearly admits a classically efficient parametrisation in terms of the strings  $x = (x_1, x_2)$  composed of  $O(n^2)$  bits. For  $n=1$  we have, for example, thirty six frame elements.

As before, note that  $\text{tr}[OF_x] = \langle\psi_{x_2}|O|\psi_{x_1}\rangle$  can be efficiently computed if the observable  $O$  is a Pauli operator [8, 30]. In addition, Eq. (22) is satisfied as  $|\langle\psi_{x_2}|O|\psi_{x_1}\rangle| \leq \|O\|$ . Consider now Eqs. (15)-(16) which take the form

$$\rho_0 = \sum_{x \in \mathcal{X}^{(0)}} \lambda_x^{(0)} |\psi_{x_1}\rangle\langle\psi_{x_2}|, \quad (35)$$

$$\mathcal{C}_j(|\psi_{x_1}\rangle\langle\psi_{x_2}|) = \sum_{y \in \mathcal{X}_x^{(j)}} \lambda_{x,y}^{(j)} |\psi_{y_1}\rangle\langle\psi_{y_2}|. \quad (36)$$

For an initial stabilizer state such as  $\rho_0 = |0^n\rangle\langle 0^n|$ , a trivial decomposition exists where  $\mathcal{X}^{(0)}$  contains a single element and  $\|\lambda^{(0)}\|_1 = 1$ .

Regarding the decomposition of gates, the discussion is analogous to the diagonal case. Since Clifford unitaries map stabilizer states to stabilizer states, they also map dyadic frame elements to dyadic frame elements. Therefore, if a channel  $\mathcal{C}_j$  can be written as a convex combination of poly( $n$ ) unitary Clifford channels then one can efficiently find a decomposition (36) where  $\mathcal{X}_x^{(j)}$  contains

polynomially many elements and  $\|\lambda_x^{(j)}\| = 1$  by the same argument as before.

As discussed previously, for general non-Clifford channels  $\mathcal{C}_j$  one can, without loss of generality, consider the action of a single-qubit channel  $\mathcal{C}_j = \mathcal{I}^{\otimes(n-1)} \otimes \mathcal{C}'_j$  on the last qubit of the system. We are interested in finding decompositions of the form (36) for such a channel  $\mathcal{C}_j$  having the lowest possible  $\|\lambda^{(j)}\|_1$ . Similarly to Eq. (31) we can write  $\mathcal{C}_j(|\psi_{x_1}\rangle\langle\psi_{x_2}|)$  as

$$\begin{aligned} \mathcal{C}_j(|\psi_{x_1}\rangle\langle\psi_{x_2}|) &= (C_1^{(n-1)} \otimes 1) \\ &\times \left[ |0^{n-2}\rangle\langle 0^{n-2}| \otimes (\mathcal{I} \otimes \mathcal{C}'_j)(|\psi_1^{(2)}\rangle\langle\psi_2^{(2)}|) \right] (C_2^{(n-1)} \otimes 1)^\dagger \end{aligned} \quad (37)$$

where  $|\psi_1^{(2)}\rangle$  and  $|\psi_2^{(2)}\rangle$  are 2-qubit stabilizer state vectors, and  $C_1^{(n-1)}$  and  $C_2^{(n-1)}$  are Clifford unitaries acting on  $n-1$  qubits. Thus, any decomposition of  $\mathcal{C}_j(|\psi_1^{(2)}\rangle\langle\psi_2^{(2)}|)$  over 2-qubit dyadic stabilizer elements  $\{|\psi_{y_1}^{(2)}\rangle\langle\psi_{y_2}^{(2)}|\}$  will also give a decomposition of  $\mathcal{C}_j(|\psi_{x_1}\rangle\langle\psi_{x_2}|)$  with the same value of  $\|\lambda_x^{(j)}\|_1$ , by substituting it into equation (37). Similarly, for channels acting on a constant number of qubits  $q$ , one can restrict the optimization to dyadic frame elements of  $q+1$  qubits. As before, solutions to this restricted problem turn out to be optimal also for the generic one. In summary, the optimization problem can be efficiently solved also in this case, as we discuss more in detail in the next section.

## 3. Optimal decompositions for stabilizer frames

Let us now analyse in more detail the concrete results that can be obtained for the simulation of noisy gate-sets with the stabilizer frames introduced above. We focus here on a standard gate-set composed of arbitrary unitary Clifford gates supplemented by the magic gate  $T = \sqrt[4]{Z}$ . We further model the presence of noise in the system by assuming that each such gate is followed by single-qubit Pauli noise channels acting on the same qubits as the gate.

As argued in the previous sections, the Clifford gates are efficiently simulable in both the diagonal and dyadic stabilizer frames and, assuming Pauli noise, this remains true also in the noisy case. We can thus concentrate on examining the cost of simulating the noisy  $T$ -gates. As a concrete example, we consider then the channel  $\mathcal{C}_{T,\text{depol.}}(\cdot) = \mathcal{N}_p^{\text{depol.}}(T(\cdot)T^\dagger)$ , given by a  $T$ -gate followed by depolarising noise of strength  $p$ , where

$$\mathcal{N}_p^{\text{depol.}}(\rho) := (1-3p)\rho + p(X\rho X + Y\rho Y + Z\rho Z). \quad (38)$$

As discussed in the previous sections, this means that we need to numerically find optimal decompositions of the 2-qubit operator

$$(\mathcal{I} \otimes \mathcal{N}_p^{\text{depol.}})(\mathbb{1} \otimes T |\psi_1^{(2)}\rangle\langle\psi_2^{(2)}| \mathbb{1} \otimes T^\dagger), \quad (39)$$

for arbitrary 2-qubit stabilizer state vectors  $|\psi_1^{(2)}\rangle, |\psi_2^{(2)}\rangle$  (for the diagonal frame it is sufficient to consider  $|\psi_1^{(2)}\rangle = |\psi_2^{(2)}\rangle$ ). For the diagonal stabilizer frame, which is Hermitian, finding a stabilizer decomposition with minimal  $\|\lambda\|_1$  is the well-known basis pursuit problem, which can be phrased as a linear program. For the more general dyadic stabilizer frame, which allows for complex coefficients, the optimization can be phrased as a second-order cone problem.

In particular, let  $y \in \mathbb{C}^{16}$  be the vector representation of the operator (39) in the 16-dimensional Pauli basis of two qubit operators. Furthermore, consider the matrix  $D \in \mathbb{C}^{16 \times |\mathcal{X}^{(2)}|}$  whose columns are the vector representations, in the same Pauli basis, of all 2-qubit frame elements (that is of all objects  $|\psi_x^{(2)}\rangle\langle\psi_x^{(2)}|$  in the diagonal case and  $|\psi_{x_1}^{(2)}\rangle\langle\psi_{x_2}^{(2)}|$  in the dyadic case). Here,  $|\mathcal{X}^{(2)}|$  is the dimension of this 2-qubit frame (*i.e.*, 60 in the diagonal case and 3600 in the dyadic case). Then, for every possible value of  $y$  (that is, for the value of expression (39) corresponding to every choice  $|\psi_1^{(2)}\rangle\langle\psi_2^{(2)}| \in \mathcal{X}^{(2)}$ ), we need to solve the optimization problem

$$\begin{aligned} \min_{\lambda \in \mathbb{C}^{|\mathcal{X}^{(2)}|}} \quad & \|\lambda\|_1 \\ \text{s.t.} \quad & D\lambda = y. \end{aligned} \quad (\mathbf{P1})$$

One can show that the problem **P1** can be reformulated as the equivalent problem **P2** given by

$$\begin{aligned} \min_{x \in \mathbb{R}^{3I}} \quad & (\mathbf{1} \ 0 \ 0) x \\ \text{s.t.} \quad & \begin{pmatrix} \mathbf{0} & & \\ \text{Re}(D) & -\text{Im}(D) & \\ \text{Im}(D) & \text{Re}(D) & \end{pmatrix} x = \begin{pmatrix} \mathbf{0} \\ \mathbf{0} \\ y \end{pmatrix} \\ & \|(\pi_{I+i} + \pi_{2I+i})x\|_2 \leq e_i^T x \\ & i = 1, \dots, I, \end{aligned} \quad (\mathbf{P2})$$

where  $\pi_i = e_i e_i^T$ ,  $I = |\mathcal{X}^{(2)}|$ , and  $\|\cdot\|_2$  is the Euclidean vector 2-norm. This is now a canonical formulation of a second-order cone program which can be solved with standard solver implementations [31], efficiently in  $|\mathcal{X}^{(2)}|$ .

Furthermore, note that by virtue of Lagrange duality [32] one can also in principle obtain certificates of optimality for the solutions of **P2** by solving the dual problem [33]

$$\begin{aligned} \max_{\nu, \{t_i, u_i\}} \quad & (\mathbf{0} \ \mathbf{0} \ y) \nu \\ \text{s.t.} \quad & A^T \nu + \sum_{i=1}^I (t_i e_i + M_i^T u_i) = (\mathbf{1} \ \mathbf{0} \ \mathbf{0})^T, \quad (40) \\ & \|u_i\|_2 \leq t_i, \quad i = 1, \dots, I, \end{aligned}$$

where  $A$  is the matrix in the equality constraint of **P2**, and  $M_i = \pi_{I+i} + \pi_{2I+i}$ . Indeed, every solution of the Lagrange dual maximization problem provides a proven lower bound on **P2**; thus, equality of both solutions can

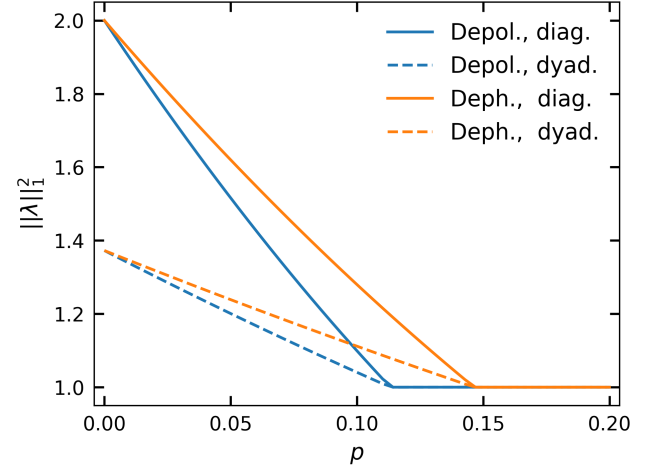


FIG. 2. **Stabilizer frames.**  $\|\lambda^{(j)}\|_1^2$  for optimal decompositions in the diagonal and dyadic stabilizer frames of the noisy  $T$ -gate at different depolarizing and dephasing strengths  $p$ . The total algorithm runtime will scale as  $O(\|\lambda\|_1^{2t})$ , where  $t$  is the number of noisy  $T$  gates in the circuit.

be used as a guarantee of optimality. Problems of this kind are hence more than helpful formulations for numerical approaches, but they can equally be used in rigorous proofs.

Figure 2 shows the results of our optimization. We plot (solid blue line) the maximal value of  $\|\lambda_x^{T,\text{depol.}}\|_1$  over all input stabilizer frame elements for the channel  $\mathcal{C}_{T,\text{depol.}}$  as a function of the noise strength  $p$ . First of all, we notice that an inverse threshold behaviour is visible. That is, the noisy  $T$ -gate can be simulated efficiently in these frames if the noise strength exceeds a certain critical value  $p_{\text{cl}} \approx 0.11$ , above which  $\|\lambda\|_1 = 1$ . This is not surprising as it is known that above this value the depolarized  $T$ -gate is equivalent to a convex combination of Clifford channels, which can be simulated efficiently [34].

Then, we observe that using the more generic dyadic frame (dashed blue line) gives a significant improvement in the simulation cost at low depolarizing strength  $p$  over the diagonal frame. Nonetheless, even with this improved frame, the threshold value remains fixed at the same point where the noisy gate becomes a Clifford operation. We will explain this last fact in Section IV C, showing that theorems based on magic-state distillation imply that a lower inverse threshold would be impossible for stabilizer frames.

Finally, we can compare these results to the performance of state-of-the-art methods for the simulation of noiseless Clifford+ $T$  circuits, known as *stabilizer extent* methods [7, 8]. These methods can be naively extended to the simulation of circuits with Pauli noise by viewing the noisy circuit as an average over pure state trajectories, each containing additional Pauli operators. The best known algorithms of this type scale as  $1.17^t$ , where  $t$  is the number of (noisy)  $T$ -gates in the circuit. We

see that, at low noise rates, this represents a quadratic improvement over our results with the stabilizer frames. This can be traced back to some technical tools used in Ref. [7] which strongly rely on the pure state nature of the problem (which in particular allows to compute  $\langle \psi | O | \psi \rangle$  in a time proportional to  $|\psi\rangle$ 's stabilizer extent  $\xi$ , rather than the naively expected  $\xi^2$ ). On the other hand, the pure state nature of these methods also implies that they cannot benefit from the presence of noise, meaning that at larger noise strengths our methods become optimal.

We conclude by noting that the same analysis can be repeated for arbitrary Pauli noise. As an example, in Figure 2 we also plot (orange lines) the case of dephasing noise

$$\mathcal{N}_p^{\text{deph.}}(\rho) := (1-p)\rho + pZ\rho Z, \quad (41)$$

corresponding to the noisy channel  $\mathcal{C}_{T,\text{deph.}}(\cdot) = \mathcal{N}_p^{\text{deph.}}(T(\cdot)T^\dagger)$ .

## B. Product state frame

In addition to the stabilizer-based frames described in Section IV A, alternative frames suitable for Schrödinger picture simulation can be constructed from *matrix product states* (MPS) with low bond dimension  $D$ . The simplest starting point is  $D = 1$ , corresponding to product state frame  $\mathcal{F} = \{F_x\}$  with

$$F_x = \bigotimes_{k=1}^n |\psi_x^{(k)}\rangle\langle\psi_x^{(k)}|. \quad (42)$$

Here, the tensor product runs over all qubits and each local factor  $|\psi_x^{(k)}\rangle\langle\psi_x^{(k)}|$  is an element of a specific subset of normalized single-qubit states. Every product state in the frame can be specified using  $\mathcal{O}(n)$  real parameters  $x$ . Additionally, for any Pauli or product operator  $O$ , the expectation  $\text{tr}(O \bigotimes_k |\psi_x^{(k)}\rangle\langle\psi_x^{(k)}|)$  can be efficiently computed and the bound (22) is satisfied, since  $\prod_k |\langle\psi_x^{(k)}| O |\psi_x^{(k)}\rangle| \leq \|O\|$ . This makes the frame suitable for Schrödinger picture simulation.

While one may in general consider a continuous frame that includes all product states, we choose here instead a subset of finite cardinality  $|\mathcal{X}|$ . More specifically, we select a finite set of uniformly random single-qubit states from which to pick the local factors  $|\psi_x^{(k)}\rangle$ , in order to approximate the continuous set of all product states. This discretization enables a tractable numerical treatment, guaranteeing in particular that we can efficiently sample from the respective quasi-probability distributions. For an initial product state such as  $\rho_0 = |0^n\rangle\langle 0^n|$ , a trivial decomposition in the frame exists containing a single element and with  $\|\lambda^{(0)}\|_1 = 1$ , provided the state vector  $|0\rangle$  is included in our finite set of single-qubit states.

Regarding the decomposition of channels, we observe that separable channels, *i.e.*, channels whose Kraus operators factorize as  $K^{(i)} = \bigotimes_k K_k^{(i)}$ , map product states

to convex combinations of product states. Consequently, any separable channel can be efficiently simulated in the full product state frame (and we expect a similar behaviour also for the discrete approximation with finite  $|\mathcal{X}|$ ). Entangling gates, on the other hand, are not necessarily efficient to simulate with this frame.

In general, consider a channel  $\mathcal{C}_j$  acting on a constant number  $q$  of qubits (in the examples that follow this will be at most  $q = 2$ ). If, for instance, it acts non-trivially only on the first  $q$  qubits, we can write it as  $\mathcal{C}_j = \mathcal{C}'_j \otimes \mathcal{I}^{n-q}$  (for gates acting on other subsets of qubits the discussion follows analogously). In this setting it is clear that one can restrict the search for gate decompositions to the  $q$  tensor factors where the gate has acted. That is, equation (21) reduces to

$$\mathcal{C}'_j \left( \bigotimes_{k=1}^q |\psi_x^{(k)}\rangle\langle\psi_x^{(k)}| \right) = \sum_{y \in \mathcal{X}^{(q)}} \lambda_{x,y}^{(j)} \bigotimes_{k=1}^q |\psi_y^{(k)}\rangle\langle\psi_y^{(k)}|, \quad (43)$$

where  $\mathcal{X}^{(q)}$  parametrizes the set of all  $q$ -qubit product states constructed from our finite set of normalized single-qubit states. Note that equation (43) now relates operators on a system of constant size  $q$  and similarly the size of the set  $\mathcal{X}^{(q)}$  is constant. This means that it is possible to efficiently characterize the set of coefficients  $\lambda_{x,y}^{(j)}$  and find the choice that minimizes  $\|\lambda^{(j)}\|_1$ .

We can indeed proceed as we did in Section IV A 3 for stabilizer frames. Let  $y \in \mathbb{C}^{4^q}$  be the vector representation of the left-hand side of equation (43) in the Pauli basis of  $q$ -qubit operators. Furthermore, consider the matrix  $D \in \mathbb{C}^{4^q \times |\mathcal{X}^{(q)}|}$ , whose columns are the vector representations in the same Pauli basis of all  $q$ -qubit product state frame elements. Then, for all the values of  $y$ , corresponding to the left-hand side of (43) for each choice of  $\bigotimes_{k=1}^q |\psi_x^{(k)}\rangle\langle\psi_x^{(k)}|$  in the frame, we need to solve the optimization problem

$$\begin{aligned} \min_{\lambda \in \mathbb{C}^{|\mathcal{X}^{(q)}|}} \quad & \|\lambda\|_1 \\ \text{s.t.} \quad & D\lambda = y. \end{aligned}$$

As discussed previously, this can be mapped to the second-order cone program P2 and solved efficiently.

In Figure 3 we show the results of this optimization for a universal gate-set composed of the single-qubit Hadamard ( $H$ ) and magic ( $T$ ) gates, as well as the two-qubit controlled-NOT ( $CNOT$ ) gate, where each gate is followed by a depolarizing noise channel (38) on all qubits that it acts on. Here, we choose a discrete set of local single-qubit states of size 30, *i.e.*,  $|\mathcal{X}^{(2)}| = 30^2$ . The figure shows the maximal value of  $\|\lambda_x^{(j)}\|_1$  across all inputs  $x \in \mathcal{X}$ , for the channels in our gate set, plotted as a function of the depolarizing strength  $p$ . Consistent with the behaviour observed for stabilizer-based frames in Section IV A, we again find an inverse threshold at approximately  $p_{\text{cl}} \approx 0.11$ . Above this threshold, the condition  $\|\lambda^{(j)}\|_1 = 1$  holds, and all circuits composed of

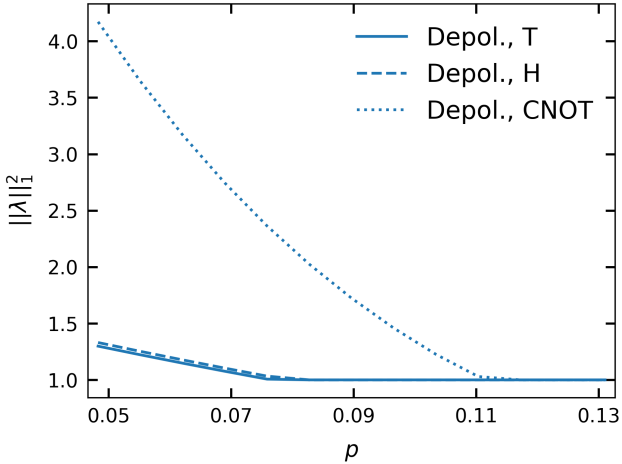


FIG. 3. **Product frame.**  $||\lambda^{(j)}||_1^2$  for optimal decompositions with respect to a discrete approximation of the continuous product-state frame, plotted as a function of the depolarizing strength  $p$  for the three gates in the gate-set ( $H$ ,  $T$ , and  $CNOT$ ). The frame is constructed from local factors selected from a finite set of 30 uniformly random single-qubit states.

these gates can be efficiently simulated. The fact that the single-qubit gates  $H$  and  $T$  exhibit values  $||\lambda^{(j)}||_1 > 1$  for small  $p$  is due to our discrete approximation of the continuous product state manifold.

Note that, although the  $CNOT$  gate is maximally entangling, its noisy counterpart  $\mathcal{C}_{CNOT, \text{depol.}}(\cdot) = (\mathcal{N}_p^{\text{depol.}} \otimes \mathcal{N}_p^{\text{depol.}})[CNOT(\cdot)CNOT^\dagger]$  is known to become separable once the depolarizing strength  $p$  is sufficiently large. As shown in Ref. [35], this occurs for  $p \geq (8 - \sqrt{8})/28 \approx 0.185$ . In this regime, the gate-set can be trivially simulated. For smaller noise strengths  $p \lesssim 0.185$ , the channel  $\mathcal{C}_{CNOT, \text{depol.}}$  is not separable. What our results show is that for  $0.11 \lesssim p \lesssim 0.185$  it is nevertheless separability-preserving – that is, it maps all input product states to convex combinations of product states, leading to  $||\lambda^{(j)}||_1 = 1$  and hence to efficient simulability.

### C. No-go theorems from magic distillation

When analysing stabilizer frames in Section IV A, we observed a simulability threshold  $p_{\text{cl}} \approx 0.11$  that was apparently independent of the frame choice. This fact can be explained by a striking observation first made by Reichardt in Ref. [36]. There, he showed that the following statement is true. Any algorithm that is able to simulate circuits composed of noiseless adaptive Clifford gates and noisy  $T$ -gates, with noise rate below a certain threshold, is also able to simulate universal quantum computation.

In this context, the term *adaptive Clifford gates* refers to  $q$ -qubit unitary Clifford gates which are applied conditioned on the classical outcome of a Pauli measurement

on another qubit. One can collectively see this operation as a non-unitary quantum channel  $\mathcal{C}$  applied to  $q+1$  qubits. It is not hard to see that our stabiliser frame algorithms are able to efficiently simulate these noiseless adaptive Clifford channels, similarly to the case of regular Clifford gates. For what concerns the noise threshold mentioned above, this is referred to as the *magic distillation threshold* and for depolarised  $T$ -gates is known to be  $p_{\text{dist}} = (6 - 2\sqrt{2})/28 \approx 0.11$  [36, 37]. We conclude that, if the stabiliser frame algorithms were able to efficiently simulate the noisy  $T$ -gate at noise strengths lower than  $p_{\text{dist}} \approx 0.11$ , then they would also be able to efficiently classically simulate universal quantum computation, which we do not believe to be possible. In this sense, the thresholds  $p_{\text{cl}} \approx 0.11$  observed for the stabiliser frame methods are optimal.

The statement of Reichardt above is proven by observing that circuits composed of noiseless adaptive Clifford gates and noisy  $T$ -gates below the distillation threshold can be used to efficiently simulate arbitrary universal quantum computations [38]. Indeed, if one has access to noisy  $T$ -gates, one can use them to create noisy approximations of the  $T$ -state vector  $|T\rangle = T|+\rangle$ . The fact that the noise rate is below the distillation threshold then implies that a logarithmically large number of these noisy  $T$ -state can be combined, using a circuit of noiseless adaptive Clifford gates, to produce (or *distil*) an arbitrarily good approximation of the ideal  $T$ -state. This  $T$ -state can then be used to perform magic state injection (again by using a noiseless adaptive Clifford circuit) and reproduce the action of the noiseless  $T$ -gate, which is the only missing element to achieve universality with the considered gate-set.

One may wonder if an analogous result can be derived from the concept of *entanglement distillation*, which would be applicable to the product state frame discussed in Section IV B. Consider, indeed, a model where each circuit qubit is interpreted as a local party, who is allowed to perform arbitrary adaptive local gates. One can verify that these adaptive local gates are efficiently simulable by a frame composed of product states. Suppose then that we supplement this model with the possibility of performing noisy entangling gates between the local parties. If the noise on these gates is below the entanglement distillation threshold, then the parties could use adaptive local operations to distil noiseless Bell pairs between them. These Bell states could then be used in a gate teleportation protocol to implement noiseless entangling gates and achieve universal quantum computation. This reasoning would imply that the product frame algorithms should not be able to efficiently simulate noisy entangling gates below the entanglement distillation threshold.

However, we encounter here a difficulty in this analysis. Indeed, in order for two local parties to be able to perform Bell state distillation, they need to be able to hold at least two shared noisy Bell pairs. This means that each local party needs to have a local Hilbert space dimension large enough to hold the local halves of at least

two Bell states, plus possible further ancillary degrees of freedom necessary for the gate teleportation protocol. However, in the model discussed above, the local parties only hold a single circuit qubit, which is clearly not enough for this. In conclusion, it seems that an analysis based on entanglement distillation can only constrain the power of product state frames if the local dimension of these states is large enough, while no bounds are known for the qubit case discussed in Section IV B. It is an open question whether bounds for qubit states can be derived in this way.

## V. RESULTS IN THE HEISENBERG PICTURE

We now consider algorithms constructed with choices of frames suitable for the Heisenberg picture simulation. An appealing feature of these algorithms is that they can overcome the limitations discussed in Section IV C. This is in particular true, as we discuss in more detail below, for the Pauli frame methods, which have enjoyed significant attention in the recent literature [11–16]. We therefore begin by discussing the Pauli method from the frame theory point of view, giving a new perspective on its good simulation power. We then show that these Pauli-based algorithms are actually still not optimal. We are indeed able to introduce an extension of the Pauli frame which exhibits an improved simulation threshold.

### A. Pauli frame

If we choose the Pauli operator basis as our frame, we construct a simulation algorithm closely related to the well-known Pauli back-propagation methods. More precisely, we consider here the frame  $\mathcal{F} = \{F_x\}_{x \in \mathcal{X}}$ , where the frame elements  $F_x = P_x$  are Pauli operators, that is tensor products of the local Pauli matrices  $\{I, X, Y, Z\}$ . Each element  $F_x$  can therefore be labelled by a string  $x$  of  $2n$  bits, which provides an efficient parametrisation of the frame. It also follows that the frame size is  $|\mathcal{X}| = 4^n$ .

First, we notice that  $\text{tr}[\rho_0 P_x]$  can be efficiently computed for  $\rho_0 = |0^n\rangle\langle 0^n|$  and in general for initial states that are stabilizer states or product states. Furthermore equation (26) is always satisfied with  $|\text{tr}[\rho_0 P_x]| \leq 1$  for all  $x$ . This makes the frame suitable for simulation in the Heisenberg picture. We therefore move on to study equations (24)–(25), which take the form

$$O = \sum_{x \in \mathcal{X}^{(0)}} \lambda_x^{(0)} P_x, \quad (44)$$

$$\mathcal{C}_j^*(P_x) = \sum_{y \in \mathcal{X}_x^{(j)}} \lambda_{x,y}^{(j)} P_y. \quad (45)$$

The decomposition (44) gives  $\|\lambda_0\|_1 = 1$  whenever  $O$  is a Pauli observable. This corresponds to a trivial decomposition where  $\mathcal{X}^{(0)}$  contains a single element.

Regarding the decomposition of gates (45), note that the Pauli operators form an orthogonal basis, therefore the decomposition can be uniquely identified as

$$\lambda_{x,y}^{(j)} = \frac{1}{2^n} \text{tr}[P_y \mathcal{C}_j^*(P_x)] \quad (46)$$

and is thus related to the so-called *Pauli transfer matrix* of the channel. In particular, if  $\mathcal{C}_j^*$  is a local channel with support on a constant number of qubits, then the expression above is non-zero only for a constant number of indices  $y$ , that is the ones such that  $P_y$  differs from  $P_x$  only on the tensor factors where the gate acts. For these relevant indices  $y$ , the coefficient  $\lambda_{x,y}^{(j)}$  can be evaluated efficiently, as this reduces to a computation in terms of local operators.

Furthermore, if a channel  $\mathcal{C}_j^*$  can be written as a convex combination of  $\text{poly}(n)$  Clifford channels then (45) takes a form where  $\mathcal{X}_x^{(j)}$  contains polynomially many elements and  $\|\lambda_x^{(j)}\| = 1$ . More specifically, consider

$$\mathcal{C}_j^*(\cdot) = \sum_k p_k C_k^\dagger(\cdot) C_k, \quad (47)$$

where  $C_k$  are Clifford unitaries. Then, because Cliffords map Pauli operators into Pauli operators, equation (45) is satisfied by a choice where the coefficients  $\lambda_{x,y}^{(j)}$  coincide with the positive normalised distribution  $p_k$ . It follows that this class of channels can be simulated with an efficient algorithm cost. For example, this applies to any local Clifford gate affected by Pauli noise.

On the other hand, channels  $\mathcal{C}_j^*$ , which do not correspond to a Clifford operation, may in general have  $\|\lambda_x^{(j)}\| > 1$  and contribute to an inefficient simulation cost. Consider for instance a noiseless  $T$ -gate. We have

$$T^\dagger X T = \frac{1}{\sqrt{2}}(X + Y), \quad (48)$$

which means that, for any Pauli operator  $P_x$  which contains an  $X$  factor on the qubit where the  $T$ -gate is acting,  $\mathcal{C}_j^*(P_x) = (P_x + P'_x)/\sqrt{2}$ . Here  $P'_x$  is the same Pauli string as  $P_x$ , where the  $X$  factor was replaced by a  $Y$ . This corresponds to a decomposition (45) where  $\lambda_{x,y}^{(j)}$  takes two different non-zero values and  $\|\lambda_x^{(j)}\| = \sqrt{2} > 1$ .

In the case of noisy non-Clifford gates, the specific value of  $\|\lambda_x^{(j)}\|$  will depend on the interplay between the unitary gate and the strength of the noise. In Figure 4 (solid line), we plot the value of  $\|\lambda^{T,\text{depol.}}\|_1$  for the channel  $\mathcal{C}_{T,\text{depol.}}(\cdot) = \mathcal{N}_p^{\text{depol.}}(T(\cdot)T^\dagger)$ , that is a  $T$ -gate followed by depolarising noise of strength  $p$ , as defined in (38). Note that here, as the Pauli frame is also a basis, there is no need to optimize over possible channel decompositions: the plotted results are derived directly by computing (46) for the given channel. We observe also in this case an inverse threshold behaviour. In the Pauli frame, the Clifford+ $T$  gate-set becomes classically simulable above a critical noise strength  $p_{\text{cl}} \approx 0.07$ , considerably lower than the corresponding threshold in the stabiliser-based frames discussed in Section IV A.

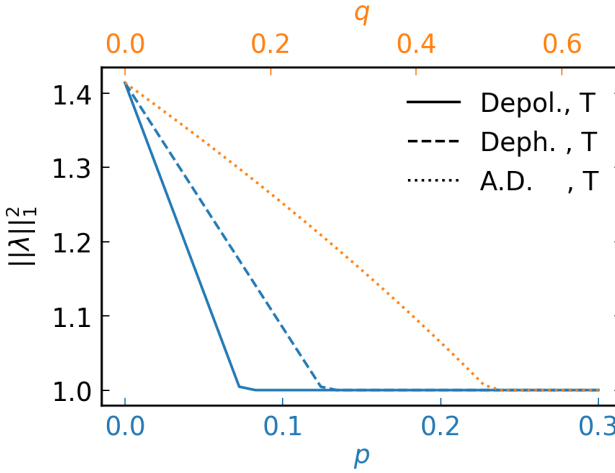


FIG. 4. **Pauli frame.**  $\|\lambda^{(j)}\|_1^2$  for decompositions in the Pauli frame of the noisy  $T$ -gate at different depolarizing, dephasing and amplitude damping (A.D.) strengths. Note that the depolarizing and dephasing strengths  $p$  and the amplitude damping strength  $q$  are plotted in separate axes as they take values in different ranges.

It may seem surprising, given the discussion in Section IV C, that the Pauli frame algorithm is able to efficiently simulate a noisy  $T$ -gate below the magic distillation threshold  $p_{\text{dist}} \approx 0.11$ . However, there is no contradiction because, as previously noticed by Rall *et al.* [39], the Pauli frame method is not able to efficiently simulate adaptive Clifford operations. Indeed, any adaptive gate has  $\|\lambda\|_1 > 1$  in this frame. In conclusion, it is precisely this limitation of the Pauli method (not being able to simulate adaptive circuits), that at the same time allows it to circumvent the no-go theorem of Section IV C and reach a lower simulability threshold.

We conclude by noting that the same observations can be repeated for other noise models. As examples, in Figure 4 we also plot the case of the dephasing noise channel (41) (dashed line) and the amplitude damping channel (dotted line), which is defined as

$$\mathcal{N}_q^{\text{A.D.}}(\rho) := K_1 \rho K_1^\dagger + K_2 \rho K_2^\dagger, \quad (49)$$

with Kraus operators

$$K_1 = \begin{pmatrix} 1 & 0 \\ 0 & \sqrt{1-q} \end{pmatrix}, K_2 = \begin{pmatrix} 0 & \sqrt{q} \\ 0 & 0 \end{pmatrix}. \quad (50)$$

Notice in particular that the latter is a non-unital channel, representing a typically more challenging form of noise to simulate than unital Pauli channels (even in average-case settings [13, 20]). It is not immediately obvious that Clifford gates perturbed by amplitude damping noise can always be simulated efficiently, however this can also be separately verified with the same analysis for this frame.

## B. Extended Pauli frame

So far, for what concerns frames applied in the Heisenberg picture, we have only considered a frame (the Pauli frame) which is also a basis. This in particular means that the decomposition (46) is unique and the corresponding norm  $\|\lambda\|_1$  directly determines the runtime of the resulting algorithm. However, we have seen in the Schrödinger picture section that it is often advantageous to exploit overcomplete frames, where the existence of many possible decompositions allows us to choose the one with the optimal one-norm value. We will now therefore discuss how to extend the Pauli basis to an overcomplete frame where one can find decompositions with a better one-norm value than in the Pauli case.

We find that a promising choice is given by the frame  $\mathcal{F} = \{F_x\}_{x \in \mathcal{X}}$  where

$$F_x = \bigotimes_{k=1}^n f_x^{(k)}. \quad (51)$$

Here the tensor product runs over all the qubits in the system and  $f_x^{(k)}$  are local operators on the  $k$ -th qubit, chosen from the following set

$$f_x^{(k)} \in \left\{ I, X, Y, Z, \frac{a}{\sqrt{2}}(X+Y), \frac{a}{\sqrt{2}}(X-Y) \right\}, \quad (52)$$

for a fixed choice of the hyperparameter  $a \in [0, 1]$ . To fully identify a frame element  $F_x$ , we need to specify each operator  $f_x^{(k)}$  among this constant number of possible choices. This means that the frame can be efficiently parametrised by a string  $x$  of  $O(n)$  bits. Notice that this is a direct generalization of the Pauli frame, which corresponds to neglecting the last two elements of the set (52), *i.e.*, setting  $a = 0$ .

First of all, we observe that, just as in the Pauli case, we still have that  $|\text{tr}[\rho_0 F_x]| \leq \|F_x\| \leq 1$  for all  $x$  and that  $\text{tr}[\rho_0 F_x]$  can be efficiently computed for  $\rho_0 = |0^n\rangle\langle 0^n|$  or any product initial state. Furthermore, if we focus on Pauli observables  $O$ , there exists always a decomposition (24) with  $\|\lambda_0\|_1 = 1$  (which just coincides with the decomposition on the Pauli basis).

For what concerns the decomposition of gates, we instead encounter a different scenario than in the Pauli case. Indeed, it is no longer true that any convex combination of Clifford unitaries automatically has  $\|\lambda^{(j)}\|_1 \leq 1$ , as the frame elements  $a(X \pm Y)/\sqrt{2}$  are not mapped to other frame elements. We thus need to carefully examine also the case of Clifford gates in our following analysis.

Consider therefore a generic channel  $\mathcal{C}_j$  acting on a constant number  $q$  of qubits (in the examples that follow this will be at most  $q = 2$ ). If, for instance, it acts non-trivially only on the first  $q$  qubits, we can write it as  $\mathcal{C}_j = \mathcal{C}'_j \otimes \mathcal{I}^{n-q}$  (for gates acting on other subsets of qubits the discussion follows analogously). We now need

to find efficient choices of the coefficients  $\lambda_{x,y}^{(j)}$  such that

$$\mathcal{C}_j^*(F_x) = \sum_{y \in \mathcal{X}} \lambda_{x,y}^{(j)} F_y \quad (53)$$

holds for each  $x$ . By comparing this with the frame definition (51), it is clear that it makes sense to consider decompositions with support on those frame elements  $F_y$  that differ from  $F_x$  only in the factors  $f_x^{(k)}$  where the gate is acting (*i.e.*, for  $k \leq q$ ). With this choice, equation (53) reduces to

$$\mathcal{C}_j'^* \left( \bigotimes_{k=1}^q f_x^{(k)} \right) = \sum_{y \in \mathcal{X}_x^{(j)}} \lambda_{x,y}^{(j)} \bigotimes_{k=1}^q f_y^{(k)}, \quad (54)$$

where we have defined  $\mathcal{X}_x^{(j)}$  as precisely those frame elements which differ from  $F_x$  only in the first  $q$  factors. As the size of the set (52) and  $q$  are both constant, also the size of  $\mathcal{X}_x^{(j)}$  is constant. Furthermore, equation (54) now relates operators on a system of constant size  $q$ . It is therefore possible to efficiently characterize the set of  $\lambda_{x,y}^{(j)}$  which satisfy it, independently of the system size  $n$ , and to find the choice which minimizes  $\|\lambda^{(j)}\|_1$ .

In particular, we proceed again as we did in Section IV A 3 for stabiliser frames. Let  $y \in \mathbb{C}^{4^q}$  be the vector representation of the left-hand side of equation (54) in the Pauli basis of  $q$ -qubit operators, and consider the matrix  $D \in \mathbb{C}^{4^q \times |\mathcal{X}^{(q)}|}$ , whose columns are the vector representations in the same Pauli basis of all  $q$ -qubit frame elements  $\bigotimes_{k=1}^q f_x^{(k)}$ . Here,  $|\mathcal{X}^{(q)}|$  is the dimension of this  $q$ -qubit frame, which is constant. Then, for all the values of  $y$ , corresponding to left-hand side of (54) for each choice of  $\bigotimes_{k=1}^q f_x^{(k)}$ , we need to solve the optimization problem

$$\begin{aligned} \min_{\lambda \in \mathbb{C}^{|\mathcal{X}^{(q)}|}} \quad & \|\lambda\|_1 \\ \text{s.t.} \quad & D\lambda = y. \end{aligned}$$

As discussed previously this can be mapped to the form (P2) and solved efficiently in the dimension of the problem (which is  $4^q \times |\mathcal{X}^{(q)}| = 4^q \times 6^q$ ).

In Figure 5, we plot the results of this optimization for a noisy gate-set composed of the Hadamard ( $H$ ) and controlled-NOT ( $CNOT$ ) Clifford gates and the standard magic gate ( $T$ ), all followed by the single-qubit depolarizing channel (38) of strength  $p$ . First of all, note that the outcome of this analysis depends on the specific choice of the hyperparameter  $a$  in the definition of the frame. Choosing a lower value for  $a$  makes the frame closer to the Pauli frame, where the Clifford gates are always efficiently simulable and the  $T$ -gate is not. Vice-versa, a higher value of  $a$  makes the simulation of the  $T$ -gate easier (as objects such as  $T^\dagger XT$  are now approximately contained in the frame), at the cost of making the Clifford gate  $CNOT$  less efficient. There exists an optimal value of  $a$  which balances this trade-off and achieves the optimal global threshold value for the complete gate-set. We

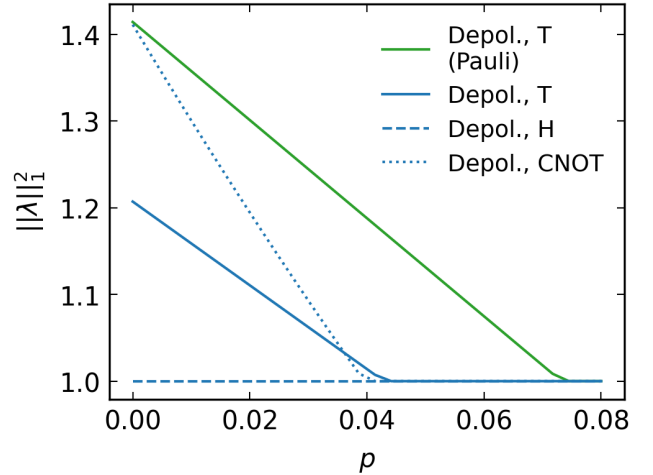


FIG. 5. **Extended Pauli frame.**  $\|\lambda^{(j)}\|_1^2$  for optimal decompositions in the extended Pauli frame at different depolarizing strengths  $p$  (blue lines). We assume a universal gate set composed of noisy Hadamard ( $H$ ), controlled-NOT ( $CNOT$ ) and magic ( $T$ ) gates. The extended Pauli frame is defined with the choice  $a = 0.84$ . For comparison we also plot the value of  $\|\lambda^{(T, \text{depol.})}\|_1^2$  for the simple Pauli frame (green line).

empirically find this value to be  $a \approx 0.84$ , which corresponds to the results shown in the figure. We observe that, with this choice of  $a$ , the extended Pauli frame gives a significantly improved simulation cost and a lower inverse threshold compared to the standard Pauli basis, at least for this gate model.

## VI. OUTLOOK

### A. A frame-based perspective on the boundary between the quantum and classical worlds

The frame-based perspective developed in this work opens up a wealth of directions for future research, both on the conceptual and on the algorithmic side. A central property of this framework is its flexibility: once a simulation problem is cast in terms of frames and quasi-probabilities, the choice of frame directly determines which quantum operations are treated as “free” and which contribute to simulation cost through their  $\|\lambda\|_1$  value. Regimes where this value is one correspond to cases where efficient classical simulation is possible, while larger values imply that quantum advantage may be possible. This approach allows a larger freedom to tackle a broader class of problems than the standard tools for “easing” the sign problem of Monte Carlo methods [22, 23, 27].

In general, it is very natural to explore frames associated with other notions of quantum resources beyond those explicitly considered here. Indeed, as we have shown for Pauli frame methods, one can substantially im-

prove on known results by more elaborate frame choices, highlighting how subtle it is to precisely delineate the boundary between the classical and quantum settings.

### B. Novel directions for frames to be explored

A particularly promising direction is to move beyond product-state frames toward frames built from weakly entangled states, such as matrix product states with bounded bond dimension. This would provide a controlled interpolation between mean-field-type simulations and those based on area-law states, making a connection with the rich literature on MPS-based classical simulation algorithms [5, 6, 40–42]. In these works, decomposition of the state are sought which minimize various measures of entanglement. Our approach would provide a different and potentially fruitful perspective where instead the focus is on the suitable one-norm quantities, according to the Monte Carlo analysis.

Similarly, frames composed of Gaussian states could be used to study the role of non-Gaussianity in noisy circuits, while frames adapted to coherence – where diagonal gates in a fixed basis are free and basis-changing gates such as Hadamard are resourceful – could offer a complementary view on coherence-based resource theories. Finally, the well-known discrete Wigner representation [17, 18] also fits naturally into our formalism, providing an example of an operator basis which, unlike the Pauli basis, is more suited for Schrödinger rather than Heisenberg picture simulation.

Looking ahead, another possible extension is the use of adaptive frames, where the frame itself is allowed to change dynamically during the simulation, depending on the gates applied or on intermediate sampling outcomes. This is analogous to the “dynamical easing of the sign problem” of standard Monte Carlo approaches. Such adaptivity could potentially reduce accumulation of sampling cost and lead to substantially improved algorithms, at the price of a more complex classical control structure. Developing systematic principles for choosing or updating frames on the fly is an open challenge. In summary, we emphasize that the frame viewpoint provides a common language for a wide class of existing and yet-to-be-developed simulation strategies.

### C. The worst-case nature of estimates

Another important aspect of our results is that they apply to concrete circuits rather than only to ensembles. The bounds derived from the frame formalism are worst-case guarantees: for any fixed circuit composed of gates from a given noisy gate-set, one can rigorously bound the simulation cost in terms of the associated one-norm. Furthermore, even when the one-norm is not known exactly, the empirical variance of the Monte Carlo estimator provides a rigorous, a posteriori diagnostic of perfor-

mance. This means that for any individual circuit one can efficiently certify whether the simulation succeeded and the reported estimates are reliable. This stands in contrast to some of the recent literature on noisy circuits focusing on *average-case simulability*, where the quantities needed to certify the success of the simulation are not always efficiently accessible [13, 20]. We anticipate this to be a powerful feature of our methods, enabling their application in a wide range of practical scenarios, where one can expect the one-norm  $\|\lambda\|_1$  to represent a simple but rather pessimistic upper-bound on the actual performance of the algorithm.

### D. Further practical and technological applications

Finally, by treating both the Schrödinger and the Heisenberg pictures, our work also contributes to clarify the relationship between different notions of simulation. While our framework is specifically tailored to the estimation of expectation values, there are specific scenarios where it can also be used for weak simulation (*i.e.*, the sampling of measurement outcomes). This is particularly the case in the Schrödinger picture simulation using frames of the form  $F_x = |\psi_x\rangle\langle\psi_x|$ , for a suitable set of states  $\psi_x$ . Here, an efficient simulation regime necessarily also corresponds to a convex representation of the evolved state in the frame, which can be used to perform weak simulation. In this context, it may also be fruitful to consider instances of “interaction picture” representations between the Schrödinger and the Heisenberg ones.

The framework presented here may find natural applications in benchmarking and verification of near-term quantum devices [43–45]. It can indeed provide classically computable reference values for the outputs of circuits with sufficiently strong noise or even of the average outputs over ensembles of noiseless circuits, which can then be used to test device performance [46]. In this context it is interesting to note that the formalism extends naturally to study higher moments and collective measurements. In particular, by considering tensor products of the analysed frames, one can straightforwardly compute multi-copy quantities that can be written as expectation values with respect to  $\rho^{\otimes q}$  for small constant  $q$  – *e.g.* purities. This paves the way to explore more advanced applications, such as monitored circuits, computations with intermediate measurements and the injection of fresh qubits. These play an increasingly important role in both experimental platforms and theoretical studies of quantum dynamics and their study will be a direction for future work.

Moving away from the circuit model, a further interesting question is to apply these methods to the dynamics of many-body systems. Here, the natural scenario would be to consider local Liouvillian dynamics, where the few-body nature of each individual Liouvillian term potentially allows for an optimization over frame representations similar to the ones considered in this work.

## VII. CONCLUSION

In this work, we have studied a unified framework for the classical simulation of noisy quantum circuits grounded in frame theory, which consolidates diverse simulation strategies within a single mathematical formalism. Simulation cost being rigorously linked to the one-norm of quasi-probability representations, this approach enables direct performance comparisons across different Schrödinger- and Heisenberg-picture methods. Exploring different frame choices led us to new and improved simulation schemes, like a generalized Pauli frame and to refined bounds on simulation efficiency that hold for individual circuits and fixed gate-sets. These results establish a rigorous, worst-case approach for deriving inverse thresholds and highlight frame theory as a powerful tool for both understanding and advancing the limits of classical simulability. On a higher level, this work helps to delineate the boundary between the noisy quantum circuits that can still be classically simulated and those for

which this is no longer possible and one can hope quantum advantages can set in. This provides a tool to assess whether *noisy intermediate scale quantum* (NISQ) computers have the potential to feature quantum utility, or whether the step to a full *fault-tolerant application-scale quantum* (FASQ) [47] computer will eventually be necessary to arrive at robust quantum utility.

## VIII. ACKNOWLEDGEMENTS

JD acknowledges the support of the Quantum Flagship PASQuanS2. JC acknowledges the support of Berlin Quantum. JE acknowledges support of the BMFTR (Hybrid++, QuSol), the Munich Quantum Valley, Berlin Quantum, QuantERA, the Quantum Flagship (Millenion, PASQuanS2), The Clusters of Excellence (MATH+, ML4Q), and the European Research Council (project DebuQC, grant agreement No. 101098279). TG acknowledges the support by the European Research Council (project DebuQC, grant agreement No. 101098279).

---

[1] C. Ferrie and J. Emerson, *New J. Phys.* **11**, 063040 (2009).

[2] C. Ferrie, *Rep. Prog. Phys.* **74**, 116001 (2011).

[3] H. Pashayan, J. J. Wallman, and S. D. Bartlett, *Phys. Rev. Lett.* **115**, 070501 (2015).

[4] J. R. Seddon, B. Regula, H. Pashayan, Y. Ouyang, and E. T. Campbell, *PRX Quantum* **2**, 010345 (2021).

[5] X. Gao and L. Duan, *Efficient classical simulation of noisy quantum computation* (2018), arXiv:1810.03176.

[6] S. Cichy, P. K. Faehrmann, L. Bittel, J. Eisert, and H. Pashayan, *Classical simulation of noisy quantum circuits via locally entanglement-optimal unravelings* (2025), arXiv:2508.05745.

[7] S. Bravyi and D. Gosset, *Phys. Rev. Lett.* **116**, 250501 (2016).

[8] S. Bravyi, D. Browne, P. Calpin, E. Campbell, D. Gosset, and M. Howard, *Quantum* **3**, 181 (2019).

[9] B. Dias and R. Koenig, *Quantum* **8**, 1350 (2024).

[10] J. Cudby and S. Strelchuk, *Gaussian decomposition of magic states for matchgate computations* (2024), arXiv:2307.12654.

[11] E. Fontana, M. S. Rudolph, R. Duncan, I. Rungger, and C. Cîrstoiu, *ant. Inf.* **11**, 84 (2025).

[12] A. Angrisani, A. Schmidhuber, M. S. Rudolph, M. Cerezo, Z. Holmes, and H.-Y. Huang, *Classically estimating observables of noiseless quantum circuits* (2024), arXiv:2409.01706.

[13] A. Angrisani, A. A. Mele, M. S. Rudolph, M. Cerezo, and Z. Holmes, *Simulating quantum circuits with arbitrary local noise using Pauli propagation* (2025), arXiv:2501.13101.

[14] Y. Shao, F. Wei, S. Cheng, and Z. Liu, *Phys. Rev. Lett.* **133**, 120603 (2024).

[15] T. Schuster, C. Yin, X. Gao, and N. Y. Yao, *A polynomial-time classical algorithm for noisy quantum circuits* (2024), arXiv:2407.12768.

[16] G. González-García, J. I. Cirac, and R. Trivedi, *Quantum* **9**, 1730 (2025).

[17] A. Mari and J. Eisert, *Phys. Rev. Lett.* **109**, 230503 (2012).

[18] V. Veitch, C. Ferrie, D. Gross, and J. Emerson, *New J. Phys.* **14**, 113011 (2012).

[19] D. Aharonov, X. Gao, Z. Landau, Y. Liu, and U. Vazirani, in *Proceedings of the 55th Annual ACM Symposium on Theory of Computing*, STOC 2023 (Association for Computing Machinery, New York, NY, USA, 2023) pp. 945–957.

[20] A. A. Mele, A. Angrisani, S. Ghosh, S. Khatri, J. Eisert, D. S. França, and Y. Quek, *Noise-induced shallow circuits and absence of barren plateaus* (2024), arXiv:2403.13927.

[21] W. Hoeffding, *J. Am. Stat. Ass.* **58**, 13 (1963).

[22] D. Hangleiter, I. Roth, Nagaj, and J. Eisert, *Science Adv.* **6**, eabb8341 (2020).

[23] J. Klassen, M. Marvian, S. Piddock, M. Ioannou, I. Hen, and B. M. Terhal, *SIAM J. Comp.* **49**, 1332 (2020).

[24] W. M. C. Foulkes, L. Mitas, R. J. Needs, and G. Rajagopal, *Rev. Mod. Phys.* **73**, 33 (2001).

[25] M. Troyer and U.-J. Wiese, *Phys. Rev. Lett.* **94**, 170201 (2005).

[26] H. Shinaoka, Y. Nomura, S. Biermann, M. Troyer, and P. Werner, *Phys. Rev. B* **92**, 195126 (2015).

[27] M. Marvian, A. Lidar, and I. Hen, *Nature Comm.* **10**, 1571 (2019).

[28] M. Howard and E. Campbell, *Phys. Rev. Lett.* **118**, 090501 (2017).

[29] D. E. Gottesman, *Stabilizer Codes and Quantum Error Correction*, Phd thesis, California Institute of Technology (1997).

[30] S. Aaronson and D. Gottesman, *Phys. Rev. A* **70**, 052328 (2004).

- [31] S. Diamond and S. Boyd, *J. Math. Learn. Res.* **17**, 1 (2016).
- [32] S. Boyd and L. Vandenberghe, *Convex optimization* (Cambridge University Press, Cambridge, 2004).
- [33] M. S. Lobo, L. Vandenberghe, S. Boyd, and H. Lebret, *Linear Algebra and its Applications* **284**, 193 (1998), International Linear Algebra Society (ILAS) Symposium on Fast Algorithms for Control, Signals and Image Processing.
- [34] H. Buhrman, R. Cleve, M. Laurent, N. Linden, A. Schrijver, and F. Unger, in *2006 47th Annual IEEE Symposium on Foundations of Computer Science (FOCS'06)* (2006) pp. 411–419.
- [35] A. W. Harrow and M. A. Nielsen, *Phys. Rev. A* **68**, 012308 (2003).
- [36] B. W. Reichardt, Quantum universality by state distillation (2009), arXiv:quant-ph/0608085.
- [37] B. W. Reichardt, *Quant. Inf. Proc.* **4**, 251 (2005).
- [38] S. Bravyi and A. Kitaev, *Phys. Rev. A* **71**, 022316 (2005).
- [39] P. Rall, D. Liang, J. Cook, and W. Kretschmer, *Phys. Rev. A* **99**, 062337 (2019).
- [40] T. Vovk and H. Pichler, *Phys. Rev. A* **110**, 012207 (2024).
- [41] Z. Chen, Y. Bao, and S. Choi, *Phys. Rev. Lett.* **133**, 230403 (2024).
- [42] A. Sander, M. Fröhlich, M. Eigel, J. Eisert, P. Gelß, M. Hintermüller, R. M. Milbradt, R. Wille, and C. B. Mendl, *Nature Comm.* **16**, 11074 (2025).
- [43] J. Eisert, D. Hangleiter, N. Walk, I. Roth, D. Markham, R. Parekh, U. Chabaud, and E. Kashefi, *Nature Rev. Phys.* **2**, 382 (2020).
- [44] J. M. Lorenz, T. Monz, J. Eisert, D. Reitzner, F. Schopfer, F. Barbaresco, K. Kurowski, W. van der Schoot, T. Strohm, J. Senellart, C. M. Perrault, M. Knufinke, Z. Amodjee, and M. Giardini, *Systematic benchmarking of quantum computers: status and recommendations* (2025), arxiv:2503.04905.
- [45] Z. Zimborás, A. Portik, D. Aguirre, R. Peña, D. Svastits, A. Pályi, A. Márton, J. K. Asbóth, A. F. Kockum, M. Sanz, O. Kálmán, T. Monz, and F. Wilhelm-Mauch, *The EU Quantum Flagship’s key performance indicators for quantum computing* (2025), arxiv:2512.19653.
- [46] F. Baccari, P. Kos, and G. Styliaris, *Average-computation benchmarking for local expectation values in digital quantum devices* (2025), arXiv:2507.18708 [quant-ph].
- [47] J. Eisert and J. Preskill, *Mind the gaps: The fraught road to quantum advantage* (2025), arXiv:2510.19928.